Effect of Impurities on the Raman Scattering of 6H-SiC Crystals

Shenghuang Lin[a]*, Zhiming Chen[a], Lianbi Li[b], Chen Yang[a]

[a]*Department of Electronic Engineering, Xi'an University of Technology, Xi'an, 710048, PR, China*
[b]*School of Science, Xi'an Polytechnic University, Xi'an, 710043, PR, China*

Raman spectroscopy was applied to different-impurities-doped 6H-SiC crystals. It had been found that the first-order Raman spectra of N-, Al- and B-doped 6H-SiC were shifted to higher frequency when comparing with undoped samples. However, the first-order Raman spectra of V-doped sample was shifted to lower frequency, revealing that there existed low free carrier concentration, which might be induced by the deep energy level effect of V impurity. Meanwhile, the second-order Raman spectra are independent of polytype and impurity type.

Keywords: *Raman scattering, 6H-SiC, impurity*

1. Introduction

Silicon carbide (SiC), one of the oldest known semiconductor materials, has received special attention in recent years because of its suitability for electronic and optoelectronic devices operating under high temperature, high power, high frequency, and/or strong radiation conditions[1-5]. As a perfect wide band gap semiconductor, SiC is an insulator whose intrinsic resistivity can be up to ~3.75×10^{21} Ω·cm. Incorporation of foreign dopants can create impurities energy levels relatively close to the conduction or valence band edges, which offers a bridge to easily excite electron (donor) or hole (acceptor) into the bands. N- or p-type SiC crystals can be achieved by doping different impurities, and the conductivity is proportional to the doping concentration when the carrier mobility is regarded as a constant. The shallower the dopant energy levels, the lower the temperature where the full dopant concentration becomes active. Nitrogen (N) or phosphorus (P) for n-type, aluminum (Al) or boron (B) for p-type and vanadium (V) for semi-insulating type, are often chosen for SiC doping. These impurities-doped SiC crystals are widely applicable. Therefore, characterization of them is essential for the development of SiC materials and devices.

In addition to other techniques, including atomic force microscopy (AFM) and scanning electron microscopy (SEM), Raman spectroscopy is becoming an increasingly common analysis method. It offers fast and contact-free measurements with easy sample preparation. Raman spectroscopy is a vibrational spectroscopy method that is based on the analysis of inelastically scattered light. The incident photons scatter of molecular vibrations (e.g., bending and rotational vibrations) or, in the case of crystals, off phonons (e.g., different modes of lattice vibration). As a result, specific spectral peak shifts occur, providing highly sensitive measurements of the material. The spectra consist of peaks that are unique in their position, shape and intensity. Usually, lasers are used as monochromatic excitation sources

and the so-called Raman shift, i.e., the energy loss (or gain) of the scattered light, is given.

Now, Raman spectroscopy has been applied to SiC material for characterizations of polytypes[6-8], stacking faults[9], stress[10] and doping[7,11,12]. In addition, it also has been employed to SiC crystals for investigating the properties in the vicinity and in the center of micropipes[13]. Especially, the Raman scattering on N-doped SiC has been reported in many papers[7,14-17]. In this case, the significant changes could be observed in the shape and position of the A_1 longitudinal optical (LO) phonon as a function of doping concentration. Meanwhile, the Raman scattering has also been employed to characterize aluminum (Al) doped 6H-SiC[17,18], the latter of which is focusing on the temperature-dependent properties. However, the effects of Al, boron (B) and vanadium (V) doping on Raman scattering are still rarely reported. Meanwhile, the difference observed from Raman scattering among these different-impurities-doped SiC crystals has not been investigated yet. In this paper, we investigate the effect of these impurities on Raman scattering at room temperature. It had been found that the Raman peaks of Al-, B-, V- and N-doped 6H-SiC shift to different frequencies, especially the peak at ~964 cm^{-1}. Then the difference among them is discussed.

2. Experimental

SiC single crystals were grown in a conventional physical vapor transport (PVT) setup[2]. Nitrogen (N) doping was performed by mixing nitrogen gas to the argon growth atmosphere. Aluminum (Al) and Boron (B) doping were achieved by the foreign impurities absorbed in the graphite crucible. Vanadium (V) doping was completed by mixing vanadium carbide (VC) to the high-purity SiC powder. The Raman spectra were measured by Renishaw inVia Raman spectrometer at room temperature using the Ar$^+$ laser of a 25 mW at 514 nm as the excitation source. All the spectral scans were performed in the range of 100~2000 cm^{-1}. The
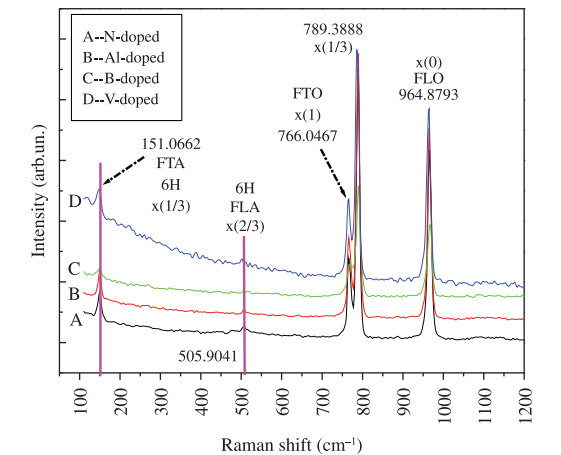
*e-mail: shenghuanglin@163.com

accuracy of the frequency measurement was better than ±1.0 cm⁻¹.
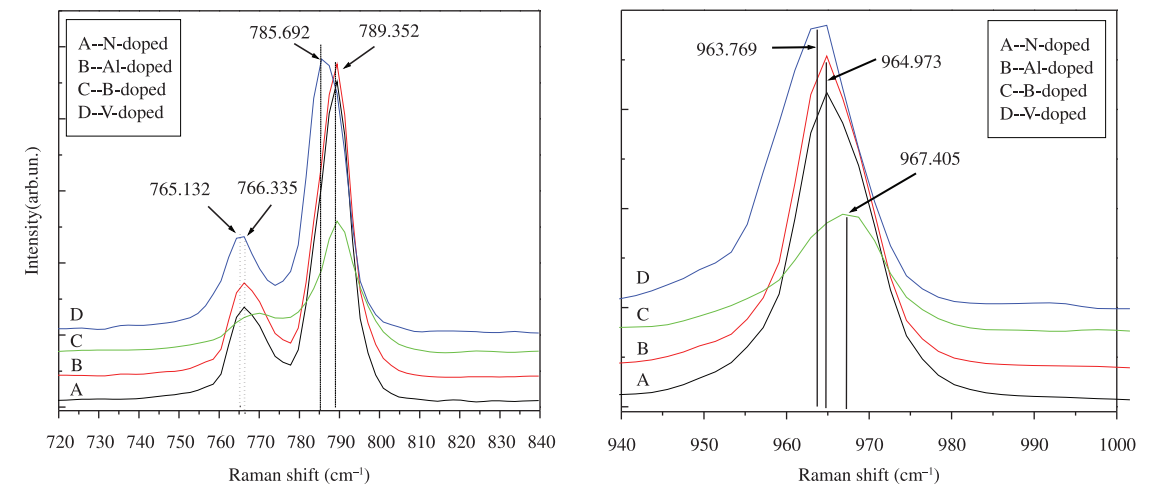
3. Results and Discussion

As we know, there are a large number of SiC polytypes for which the stacking sequences of double atomic planes of Si-C along the c-direction are different. The simplest polytype with the shortest period is the 3C polytype (β-type) which has a zincblende (cubic) structure. But one of the

Figure 1. The first-order Raman spectra of different-impurities-doped 6H-SiC samples.

two most popular polytypes is 6H polytype, which has a wurtzitic structure with C_{6v}^4 space group. And the group theory analysis predicts that the Raman active modes are of A_1 (LO) and E_1 (TO) symmetry. Due to the optical branches of A_1 and E_1 symmetry phonon modes being both Raman and IR active, they split into longitudinal and transverse branches. As the same shown in Figure 1, which reveals the first-order Raman spectra of different-impurities-doped 6H-SiC samples. It can be seen that there exist four typical peaks for FTA, FLA, FTO and FLO modes, respectively. As for the undoped 6H-SiC samples, it had been reported that these typical peaks were at 150 (FTA), 504 (FLA), 765 (FTO), 787 (FTO) and 964 (FLO) cm⁻¹, respectively[6,17]. But for impurities-doped 6H-SiC samples, the typical peaks will be quite different.

Figure 2 shows the local amplification corresponding to Figure 1 in the range of 720-1000 cm⁻¹. By a combination of Figure 2 and Table 1, it could be found that almost all the Raman peaks shifted to higher frequency except for V-doped sample. Especially for the peak of A_1 mode at ~964 cm⁻¹, it had been revealed that this peak would shift to higher frequency with the increase of carrier concentration[17]. However, the Raman peak for V-doped sample shifted to lower frequency when comparing with undoped sample. It implied that the carrier concentration in V-doped 6H-SiC was lower than that of undoped sample, revealing the conventional residual impurity N had been compensated by the deep energy level impurity V. Meanwhile, the ionization

Figure 2. Local amplification for Figure 1 in the range of 720-1000 cm⁻¹.

Table 1. Phonon modes of the different-impurities-doped 6H-SiC observed by Raman spectroscope.

	Frequency (cm⁻¹)				
	FTA	**FLA**	**FTO**	**FTO**	**LOPC**
Reference (undoped)	150	504	766	787	964
N-doped	150.731	505.976	766.612	789.352	965.106
Al-doped	150.982	506.477	766.109	789.352	964.973
B-doped	150.355	505.579	766.335	789.352	967.405
V-doped	148.516	501.463	765.132	785.682	963.769
x	0.33 (6H)	0.67 (6H)	1 (6H)	0.33 (6H)	0 (6H)

energy of V in SiC is so large that there are only few free carriers contributing to the conductivity. Therefore, the Raman frequency of V-doped SiC showed red shift due to its low carrier concentration. In order to investigate the real mechanism of this phenomenon, the principle for Raman spectroscopy is reviewed.

As we know, the spectral shape depends on the amount of plasmon damping due to carrier scattering. The line shape of the LO phonon can be written as[6,11]

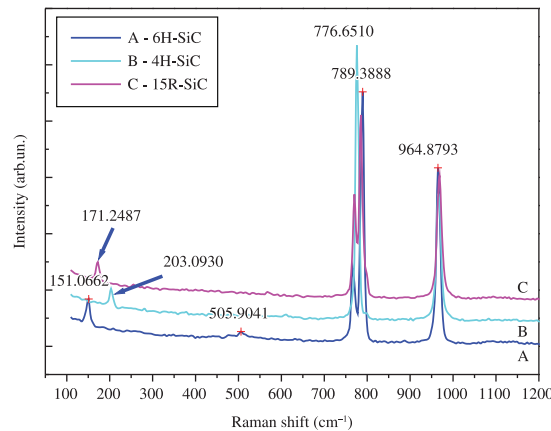$$I(\omega) = SA(\omega) \mathrm{Im}[-\frac{1}{\varepsilon(\omega)}] \tag{1}$$

where S is a proportionality constant, ω the Raman shift, $\varepsilon(\omega)$ the dielectric function, and $A(\omega)$ is given by

$$A(\omega) = 1 + \frac{2C\omega_T^2[\omega_P^2\gamma(\omega_T^2-\omega^2) - \omega^2\Gamma(\omega^2-\gamma^2-\omega_P^2)]}{\Delta}$$
$$+ \left(\frac{C^2\omega_T^4}{\Delta}\right)\left(\frac{\omega_P^2[\gamma(\omega_L^2-\omega_T^2) + \Gamma(\omega_P^2-2\omega^2)] + \omega^2\Gamma(\omega^2+\gamma^2)}{\omega_L^2-\omega_T^2}\right) \tag{2}$$

Here, ω_L and ω_T represent the longitudinal and transverse optical phonon frequencies, respectively, γ the plasmon dampening constant, Γ the phonon dampening constant,
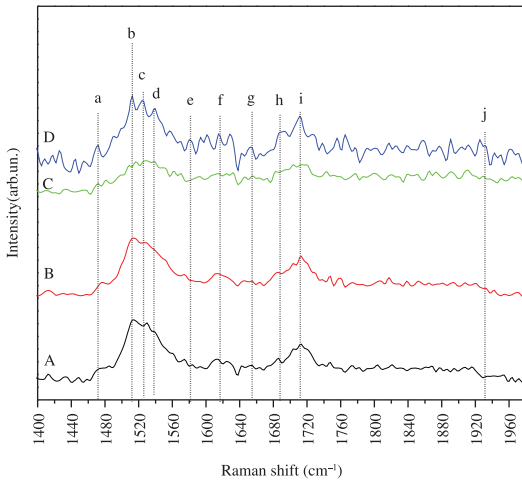
and $\Delta = \omega_P^2\gamma[(\omega_T^2-\omega^2)^2 + (\omega\Gamma)^2] + \omega^2\Gamma(\omega_L^2-\omega_T^2)(\omega^2+\gamma^2)$, and C the so-called Faust-Henry coefficient. The dielectric function $\varepsilon(\omega)$ can be expressed as $\varepsilon(\omega) = \varepsilon_\infty\left[1 + \frac{\omega_L^2-\omega_T^2}{\omega_T^2-\omega^2-i\omega\Gamma} - \frac{\omega_P^2}{\omega(\omega+i\gamma)}\right]$, which contains contribution from phonon and plasmon. And the plasmon frequency $\omega_P = (4\varpi ne^2/\varepsilon_\infty m)^{1/2}$, which is related to optical dielectric constant (ε_∞), electron effective mass (m_{eff}) and carrier density (n). The increase of the carrier density will improve the value of ω_P, and hence enhance the coupling interaction between phonons and plasmon. Then the LO phonon frequency would increase and reveal blue shift with the increase of carrier concentration. In stead, the Raman frequency would be shifted to lower wavenumber.

It is well known that the first-order Raman spectra only represent the phonons in the first Brillouin zone (Γ point) because there is only one phonon being involved. But the second-order Raman spectra show the information about the whole Brillouin zone due to two phonons participating. Figure 3 shows the second-order Raman spectra of different-impurities-doped 6H-SiC. It can be seen that the Raman peaks are labelled a (1472 cm^{-1}), b (1513 cm^{-1}), c (1526 cm^{-1}), d (1537 cm^{-1}), e (1582 cm^{-1}), f (1617 cm^{-1}), g (1655 cm^{-1}), h (1688 cm^{-1}), i (1712 cm^{-1}), j (1931 cm^{-1}). According to the selective rules for second-order scattering in hexagonal materials[19], the peaks marked as a, b, c, d, e and f are assigned to the two-phonon Raman scattering. However, there is no significant difference can be found among these different impurities doped 6H-SiC in the second-order Raman spectra. Namely, the doping concentrations have no influence on the second- order Raman scattering of SiC crystals.

In addition, the first- and second-order Raman scattering are also investigated in this paper. The first-order Raman spectra of 6H-, 4H- and 15R-SiC crystals are shown in Figure 4. The difference among these polytypes can be easily distinguished by the feature peaks of FTA mode, such as 6H- at ~151 cm^{-1}, 4H- at ~203 cm^{-1} and 15R- at ~171 cm^{-1}. However, as for the N-doped 6H-, 4H- and 15R-SiC crystals, no Raman shifts can be observed in the second-order Raman spectra (see Figure 5). Therefore, the second-order Raman scattering is independent of polytypes.

Figure 3. Second-order Raman spectra of different-impurities-doped 6H-SiC.

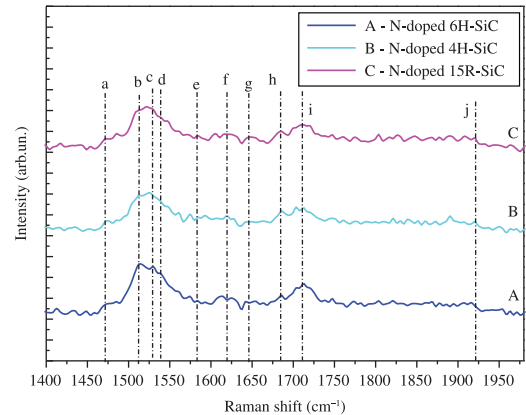**Figure 4.** First-order Raman spectra of 6H-, 4H- and 15R-SiC samples.

Figure 5. Second-order Raman spectra of 6H-, 4H- and 15R-SiC samples.

4. Conclusions

In summary, the SiC polytypes have significant effects on the first-order Raman scattering due to the existence of the folded modes. The Raman frequency and intensity of the observed peaks are polytype and doing concentration dependent. It had also been found that the Raman peaks of N-, Al- and B-doped 6H-SiC shift to high frequency, but that of V-doped sample shift to low frequency. The possible reason for this phenomenon is that the shallow energy level impurities in SiC have been compensated by the deep impurity V, resulting in low free carrier concentration. As for the second-order Raman spectra, they are nearly independent of polytype and impurities.

References

1. Lin S, Chen Z, Jiang D, Liang P, Wan J, Liu B et al. A technique for diameter enlargement in SiC crystal growth. *International Journal of Materials Research.* 2010; 101:1514-1518. http://dx.doi.org/10.3139/146.110432

2. Lin S, Chen Z, Liu B, Li L and Feng X. Identification and control of SiC polytypes in PVT method. *Journal of Materials Science Materials in Electronics.* 2010; 21:326-330. http://dx.doi.org/10.1007/s10854-009-9914-3

3. Lin S, Chen Z, Liang P, Jiang D, Xie H and Yang Y. The correlation of the results of capacitance mapping and of sheet resistance mapping in semi-insulating 6H–SiC. *Journal of Alloys and Compounds.* 2010; 489:56-58. http://dx.doi.org/10.1016/j.jallcom.2009.07.070

4. Lin S, Chen Z, Liu S, Yang Y, Feng X, Ba Y et al. Three-dimensional observation of defects in nitrogen-doped 6H-SiC crystals using a laser scanning confocal microscope. *Journal of Materials Science.* 2012; 47:3429-3434. http://dx.doi.org/10.1007/s10853-011-6190-4

5. Lin S, Chen Z, Yang Y, Liu SJ, Ba YT, Li L et al. Formation and evolution of micropipes in SiC crystals. *CrystEngComm.* 2012; 14:1588-1594. http://dx.doi.org/10.1039/c1ce05806a

6. Nakashima S and Harima H. Raman Investigation of SiC Polytypes. *Physica Status Solidi.* 1997; 162(a):39-39-64.

7. Lin S, Chen Z, Feng X, Yang Y, Li L, Wang Z et al. Observation of polytype stability in different-impurities-doped 6H–SiC crystals. *Diamond and Related Materials.* 2011; 20:516-519. http://dx.doi.org/10.1016/j.diamond.2011.02.011

8. Lin S, Chen Z, Liang P, Ba Y and Liu S. Formation and suppression of misoriented grains in 6H-SiC crystals. *CrystEngComm.* 2011; 13:2709-2713. http://dx.doi.org/10.1039/c0ce00646g

9. Nakashima S, Nakatake Y, Harima H, Katsuno M and Ohtani N. Detection of stacking faults in 6H-SiC by Raman scattering. *Applied Physics Letters.* 2000; 77:3612-3614. http://dx.doi.org/10.1063/1.1329629

10. Lu YM and Leu IC. Qualitative study of beta silicon carbide residual stress by Raman spectroscopy. *Thin Solid Films.* 2000; 377-378:389-393. http://dx.doi.org/10.1016/S0040-6090(00)01313-4

11. Burton JC, Sun L, Pophristic M, Lukacs SJ, Long FH, Feng ZC et al. Spatial characterization of doped SiC wafers by Raman spectroscopy. *Journal of Applied Physics.* 1998; 84:6268-6273. http://dx.doi.org/10.1063/1.368947

12. Lin S, Chen Z, Liang P, Jiang D and Xie H. Room-temperature ferromagnetism of vanadium-doped 6H–SiC. *Chemical Physics Letter*s. 2010; 496:56-58. http://dx.doi.org/10.1016/j.cplett.2010.07.020

13. Lin S, Chen Z, Li L, Ba Y, Liu S and Yang M. Investigation of micropipes in 6H–SiC by Raman scattering. *Physica.* 2012; B 407(4):670-673. http://dx.doi.org/10.1016/j.physb.2011.12.001 http://dx.doi.org/10.1016/j.physb.2011.12.001

14. Colwell PJ and Klein MV. Raman scattering from electronic excitations in n-type silicon carbide. *Physical Review Letters.* 1972; B 6:498-515.

15. Egilsson T, Ivanov IG, Henry A et al. Excitation spectra of nitrogen bound excitons in 4H- and 6H-SiC. *Journal of Applied Physics.* 2002; 91:2028-33. http://dx.doi.org/10.1063/1.1431437

16. Han R, Yang YT and Chai CC. Electronic Raman scattering and the second-order Raman spectra of the n-type SiC. *Acta Physica Sinica.* 2008; 57:3182-3182-3187.

17. Li XB, Chen ZZ and Shi EW. Effect of doping on the Raman scattering of 6H-SiC crystals. *Physica.* 2010; B405(10):2423-2426. http://dx.doi.org/10.1016/j.physb.2010.02.058 http://dx.doi.org/10.1016/j.physb.2010.02.058

18. Li X, Shi E, Chen Z and Xiao B. Temperature-dependent Raman Property of Al-doped 6H-SiC Crystals. *Journal of Inorganic Materials.* 2008; 23:238-42. http://dx.doi.org/10.3724/SP.J.1077.2008.00238

19. Gorban I S and Lugovoi V I. Second-order Raman scatteeing in silicon carbide crystals. *Journal of Applied Spectroscopy.* 1976; 24:233-237.